Dyes and Pigments 184 (2021) 108757

Contents lists available at ScienceDirect

Dyes and Pigments

journal homepage: http://www.elsevier.com/locate/dyepig

Solvatochromism of dyes inspired in Effenberger's probe

Carlos E.A. de Melo [a], Moisés Domínguez [b], Marcos C. Rezende [b], Vanderlei G. Machado [a,*]

[a] Departamento de Química, Universidade Federal de Santa Catarina, UFSC, Florianópolis, SC, 88040–900, Brazil
[b] Facultad de Química y Biología, Universidad de Santiago, Av. B. O'Higgins, 3363, Santiago, Chile

ARTICLE INFO

Keywords:
Solvatochromism
Reverse solvatochromism
Solvation
Solvatochromic dyes
Positive solvatochromism
Dipolarity/polarizability

ABSTRACT

Solvatochromic dyes have been utilized in recent decades as probes to measure the polarity of the medium. An interesting example is the Effenberger's dye (**ED**), which exhibits a very pronounced positive solvatochromism, being considered a dye that probes practically only the polarizability and dipolarity of the medium. This compound is difficult to be accessed and, in addition, the synthesis of dyes capable to probe the polarizability of the medium is a subject of interest. In view of this, six imine probes inspired in the molecular structure of **ED** were synthesized and characterized. Two compounds were solvatochromic and exhibit different colors in various solvents, while the other dyes exhibit a weak solvatochromism. Three probes present a behavior very similar to **ED**, showing a positive solvatochromic behavior. The application of multiparametric equations shows that polarizability is the most influential solvent parameter in the solvation of the dyes studied. Theoretical calculations were performed with a dye in ten different solvents, employing a continuum model to mimic solvent effects and TD/DFT calculations with two functionals exhibiting a different degree of Hartree–Fock exchange to estimate transition energy (E_T) values. A HOMO–LUMO transition involving an internal charge transfer from the *N*,*N*–dimethylaminophenyl electron–donor to the nitrothienyl electron–acceptor moieties of the dye was identified as the origin of the solvatochromic band. The calculated E_T values reproduce qualitatively the positive solvatochromism of the dye. The results obtained show that the easy synthesis of solvatochromic compounds, inspired in the **ED**, represents an interesting possibility in the research for novel polarizability probes.

1. Introduction

Solvatochromic compounds exhibit absorption bands in the visible (vis) region and their position and/or intensity is dependent on the nature of the solvent [1–3]. These dyes have been utilized in recent decades as probes to measure the polarity of the medium. An impressive example of a solvatochromic dye is the Reichardt pyridinium–*N*–phenolate betaine **1** (Fig. 1), whose negative solvatochromic behavior is the basis for the development of the largely known E_T (30) empirical polarity solvent scale [1,3–5]. The increase in the polarity of the medium causes a displacement of the solvatochromic band of dye **1** toward a lower maximum wavelength (λ_{max}) values.

The opposite behavior is found for dye **2**, introduced by Effenberger et al. [6,7]._ENREF_4 This probe exhibits a very pronounced positive solvatochromism, with its solvatochromic band in the vis region being shifted to increasing λ_{max} values as a response to the increase in the polarity of the solvent. In addition to positive solvatochromism, dye **2** is a compound that practically does not interact in a specific way with the medium, being considered a dye that probes practically only the polarizability and dipolarity of the solvent [6–11].

For some families of solvatochromic dyes, the occurrence of negative solvatochromism from the most polar solvents to the solvents of intermediate polarity is initially verified. A reversal in the solvatochromism, from negative to positive, is then observed with a further reduction in the polarity of the solvent. This phenomenon, named as reverse solvatochromism, is subtly verified in the classical Brooker's merocyanine (dye **3**) [12,13], being a subject of much controversy during the last decades [14–19]. This is because the change in the type of solvatochromism occurs only in the region of low polarity solvents. Compound **4** is another example of dye exhibiting reverse solvatochromism [20].

More recently, a particular family of dyes of general structures **5** and **6** has been studied [21–27], with a phenolate electron–donor conjugated with a polynitroaryl acceptor moiety. These dyes are readily accessible and are soluble in polar and nonpolar solvents, exhibiting a reversal in their solvatochromism in solvents of intermediate polarity.

---

* Corresponding author.
E-mail address: vanderlei.machado@ufsc.br (V.G. Machado).

https://doi.org/10.1016/j.dyepig.2020.108757
Received 7 May 2020; Received in revised form 22 July 2020; Accepted 3 August 2020

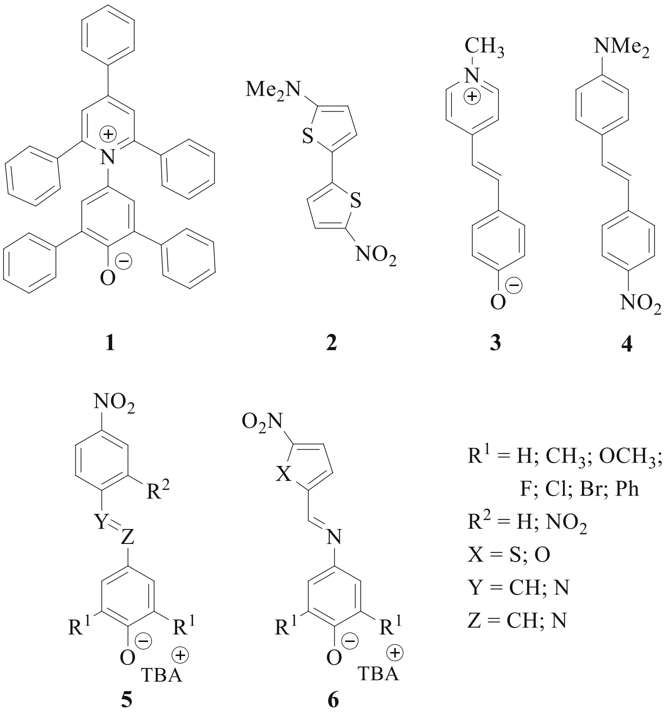

Fig. 1. Molecular structures of dyes **1**–**6** (TBA^+ = tetra–*n*–butylammonium).

Compounds exhibiting a reversal in their solvatochromism, like the compounds with the general molecular structure **5** or **6**, should belong to another category, such as class III dyes [27].

An analysis of the molecular structure of compounds **6** shows that the electron–acceptor moiety of the compounds, a heteroaromatic thiophenyl or furanyl group, is analogous to that in compound **2**. In addition, a study made with compound **4** and related dyes [20] shows that a change in the electron–donor group from phenolate (as in the case of compounds **5**) to *N,N*–dimethylaminophenyl changes their behavior with respect to their interaction with the medium. Although a reverse solvatochromism is verified for dye **4**, it is capable of acting predominantly as probe for the polarizability of the medium, with very little interference of specific interactions due to the hydrogen bonding of the solvent [20]. In addition, compounds analogous to compounds **6**, but with *N,N*–dimethylaminophenyl groups in their molecular structure, should be in principle easily obtained by simple condensation reactions, different to compound **2**, which is more difficult to synthesize [6,7]. It is also important to remark that the design of compounds capable to probe the polarizability of the medium is a subject of current interest [11, 28–33].

In view of this, herein we report the synthesis and characterization of novel imines **7**–**12** (Fig. 2), inspired in the molecular structure of probe **2**. The solvatochromism of the compounds was compared with that exhibited by dye **2**. The influence of the 5–nitro–2–thiophenyl or 5–nitro–2–furanyl electron–acceptors and of the dimethylamino, methoxy, or methylthio electron–donor groups on the solvatochromism of the systems was verified. In addition, theoretical calculations were performed with dye **7** in ten different solvents to understand the nature of the transition responsible for the solvatochromism of the dye and to reproduce qualitatively its positive solvatochromism.

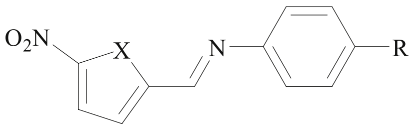

	7	8	9	10	11	12
X	S	O	S	O	S	O
R	$N(CH_3)_2$	$N(CH_3)_2$	OCH_3	OCH_3	SCH_3	SCH_3

Fig. 2. Molecular structures of dyes **7**–**12**.

2. Experimental section

2.1. Materials and methods

All reagents and solvents were analytically pure and were obtained from commercial sources (Sigma–Aldrich and Vetec). The solvents (HPLC grade) were purified following the methodology described in the literature [34,35]. Water used for all measurements was deionized, boiled, and bubbled with nitrogen and kept in a nitrogen atmosphere to avoid the presence of carbon dioxide.

NMR spectra were recorded with 200 MHz Bruker AC–200 F and with 400 MHz Bruker Avance 400 spectrometers. Chemical shifts were recorded in ppm with the solvent resonance as the internal standard and data are reported as follows: chemical shift, multiplicity (*s* = singlet, *d* = doublet, *dd* = double doublet), coupling constants (Hz), and integration. IR spectra were obtained with an FT Varian 3100 spectrometer, by using KBr pellets. High–resolution mass spectra were obtained with a Bruker OTOF–Q II 10243 electrospray ionization–quadrupole time–of–flight mass spectrometer (HR ESI–MS QTOF). The melting points were determined by means of DSC analysis, by using a Shimadzu DSC–50 apparatus. UV–vis spectra were obtained with an Agilent Technologies Cary 60 spectrometer.

2.2. Synthesis

4–Amino–*N,N*–dimethylaniline was synthesized exactly as described in literature [20]. The other amines used in the syntheses were obtained from commercial sources. Compounds **7**–**12** were synthesized according to the adapted methodology previously described [25]. The aldehyde (0.7 mmol), the amine (1 equiv), ethanol (3 mL) previously dried with molecular sieves (4 Å), and glacial acetic acid (2 drops) were mixed in a round–bottomed flask. The reaction mixtures were maintained under reflux at 78 °C for 1 h. After this period, the solid products obtained were filtered off, washed with ice–cold ethanol, dried under vacuum, and stored in vacuum desiccator over P_4O_{10}.

***N,N*–Dimethyl–*N*'–[(1*E*)–(5–nitro–2–thienyl)methylene] benzene–1,4–diamine (7)**. Compound synthesized from 5–nitro–2–thiophenecarboxaldehyde and 4–amino–*N,N*–dimethylaniline. Dark red solid (yield: 73%). M. p.: 199.2 °C. IR (KBr) $\bar{\nu}_{max}/cm^{-1}$: 3428 (intramolecular hydrogen bond of the N from the C=N); 2898 (C–H); 1560 and 1493 (N=O); 1323 (CH_3); 1162 (C–S). ^1H NMR (200 MHz, DMSO–d_6) δ/ppm: 8.84 (*s*, 1H); 8.03 (*d*, 1H, $J = 4.3$ Hz); 7.52 (*d*, 1H, $J = 4.3$ Hz); 7.37 (*d*, 2H, $J = 8.9$ Hz); 6.78 (*d*, 2H, $J = 8.9$ Hz); 3.01 (*s*, 6H). ^{13}C NMR (50 MHz, DMSO–d_6) δ/ppm: 151.0; 150.6; 150.4; 146.3; 137.3; 130.6; 129.6; 123.5; 112.3. HRMS (ESI, TOF) *m/z*: 276.0804 $[M+H]^+$, calculated for $C_{13}H_{13}N_3O_2S$, 276.0801.

***N,N*–Dimethyl–*N*'–[(1*E*)–(5–nitro–2–furanyl)methylene] benzene–1,4–diamine (8)**. Compound synthesized from 5–nitro–2–furaldehyde and 4–amino–*N,N*–dimethylaniline. Dark red solid (yield: 75%). M. p.: 180.0 °C. IR (KBr) $\bar{\nu}_{max}/cm^{-1}$: 3428 (intramolecular hydrogen bond of the N from the C=N); 2900 (C–H); 1619 (C=N); 1507 and 1472 (N=O); 1352 (CH_3); 1256 (C–O). ^1H NMR (200 MHz, acetone–d_6) δ/ppm: 8.58 (*s*, 1H); 7.62 (*d*, 1H, $J = 3.8$ Hz); 7.40 (*d*, 2H, $J = 8.9$ Hz); 7.21 (*d*, 1H, $J = 3.8$ Hz); 6.78 (*d*, 2H, $J = 8.9$ Hz); 3.02 (*s*, 6H). ^{13}C NMR (50 MHz, DMSO–d_6) δ/ppm: 166.2; 153.9; 150.0; 140.3; 137.4; 128.9; 122.9; 115.1; 114.3; 111.4. HRMS (ESI, TOF) *m/z*: 260.1033 $[M+H]^+$, calculated for $C_{13}H_{13}N_3O_3$, 260.1030.

4–Methoxy–*N*–[(1*E*)–(5–nitro–2–thienyl)methylene] aniline (9).

Compound synthesized from 5–nitro–2–thiophenecarboxaldehyde and *p*–anisidine. Bright red–orange solid (yield: 87%). M. p.: 155.6 °C. IR (KBr) $\overline{\nu}_{max}$/cm^{-1}: 3422 (intramolecular hydrogen bond of the N from the C=N); 3096 (C–H); 1609 (C=N); 1535 and 1493 (N–O); 1329 (CH_3); 1289 and 1244 (C–O); 1191 (C–S). ^{1}H NMR (200 MHz, DMSO–d$_6$) δ/ppm: 8.71 (*s*, 1H); 7.96 (*d*, 1H, $J = 4.3$ Hz); 7.47 (*d*, 1H, $J = 4.3$ Hz); 7.34 (*d*, 2H, $J = 9.0$ Hz); 6.99 (*d*, 2H, $J = 9.0$ Hz); 3.82 (*s*, 1H). ^{13}C NMR (50 MHz, DMSO–d$_6$) δ/ppm: 159.1; 150.5; 149.3; 141.9; 131.0; 130.5; 123.3; 114.6; 55.4; 18.5. HRMS (ESI, TOF) *m/z*: 263.0487 [M+H]$^+$, calculated for $C_{12}H_{10}N_2O_3S$, 263.0485.

4–Methoxy–*N*– [(1*E*)–(5–nitro–2–furanyl)methylene] aniline (10). Compound synthesized from 5–nitro–2–furaldehyde and *p*–anisidine. Bright yellow solid (yield: 80%). M. p.: 123.2 °C. IR (KBr) $\overline{\nu}_{max}$/cm^{-1}: 3424 (intramolecular hydrogen bond of the N from the C=N); 3157 (C–H); 1619 (C=N); 1529 and 1501 (N–O); 1354 (CH_3); 1297 and 1244 (C–O). ^{1}H NMR (200 MHz, DMSO–d$_6$) δ/ppm: 8.64 (*s*, 1H); 7.81 (*d*, 1H, $J = 3.9$ Hz); 7.42 (*d*, 2H, $J = 8.8$ Hz); 7.35 (*d*, 1H, $J = 3.9$ Hz); 7.01 (*d*, 2H, $J = 8.8$ Hz); 3.79 (*s*, 1H). ^{13}C NMR (50 MHz, DMSO–d$_6$) δ/ppm: 159.2; 153.3; 152.1; 145.0; 142.4; 123.2; 116.9; 114.6; 114.3; 55.4. HRMS (ESI, TOF) *m/z*: 247.0710 [M+H]$^+$, calculated for $C_{12}H_{10}N_2O_4$, 247.0713.

4–Methylthio–*N*– [(1*E*)–(5–nitro–2–thienyl)methylene] aniline (11). Compound synthesized from 5–nitro–2–thiophenecarboxaldehyde and 4–(methylthio)aniline. Bright red solid (yield: 77%). M. p.: 116.7 °C. IR (KBr) $\overline{\nu}_{max}$/cm^{-1}: 3424 (intramolecular hydrogen bond of the N from the C=N); 1605 (C=N); 1537 e 1509 (N–O); 1336 (CH_3); 1195 (C–S). ^{1}H NMR (400 MHz, $CDCl_3$) δ/ppm: 8.55 (*s*, 1H); 7.90 (*d*, 1H, $J = 4.2$ Hz); 7.35 (*d*, 1H, $J = 4.2$ Hz); 7.28 (*dd*, 2H, $J_1 = 2.0$ Hz e $J_2 = 8.7$ Hz); 7.23 (*dd*, 2H, $J_1 = 2.2$ Hz e $J_2 = 8.7$ Hz); 2.51 (*s*, 3H). ^{13}C NMR (50 MHz, DMSO–d$_6$) δ/ppm: 152.2; 148.8; 145.9; 138.0; 131.6; 130.4; 126.5; 122.3; 14.7. HRMS (ESI, TOF) *m/z*: 279.0259 [M+H]$^+$, calculated for $C_{12}H_{10}N_2O_2S_2$, 279.0256.

4–Methylthio–*N*– [(1*E*)–(5–nitro–2–furanyl)methylene] aniline (12). Compound synthesized from 5–nitro–2–furaldehyde and 4–(methylthio)aniline. Orange solid (yield: 75%). M. p.: 102.0 °C. IR (KBr) $\overline{\nu}_{max}$/cm^{-1}: 3424 (intramolecular hydrogen bond of the N from the C=N); 3073 (C–H); 1619 (C=N); 1515 and 1493 (N–O); 1352 (CH_3); 1258 (C–S). ^{1}H NMR (400 MHz, $CDCl_3$) δ/ppm: 8.41 (*s*, 1H); 7.42 (*d*, 1H, $J = 3.8$ Hz); 7.28 (*d*, 2H, $J = 9.1$ Hz); 7.22 (*d*, 2H, $J = 9.1$ Hz); 7.18 (*d*, 1H, $J = 3.8$ Hz); 2.51 (*s*, 3H). ^{13}C NMR (50 MHz, DMSO–d6) δ/ppm: 153.0; 152.2; 146.6; 146.4; 138.1; 126.6; 122.2; 117.6; 114.6; 14.7. HRMS (ESI, TOF) *m/z*: 263.0483 [M+H]$^+$, calculated for $C_{12}H_{10}N_2O_3S$, 263.0485.

2.3. UV–vis measurements

A stock solution with concentration of 7.0×10^{-3} mol L^{-1} for each compound was prepared in acetone. 24 μL of this stock solution were transferred to 5 mL volumetric flasks and after the evaporation of acetone the compound was dissolved in pure solvents. The final concentration of the resulting solutions was 4.0×10^{-3} mol L^{-1}. Then, the UV–vis spectra were collected at 25 °C. The maxima of the UV–vis spectra were calculated from the first derivative of the absorption spectrum, with a precision of ±0.5 nm, and the reproducibility was verified through the determination of two spectra for each dye in each pure solvent. The maximum wavelength (λ_{max}) values thus obtained were used to determine the E_T (dye) values in each solvent, given with a precision of ±0.1 kcal mol^{-1}, through Eq. (1) [1,5].

$$E_T \text{ (dye) / (kcal mol}^{-1}) = 28590/\lambda_{max} \text{ (nm)} \quad (1)$$

3. Calculation methods

For the regression analyses of the experimental transition energies, all constants were obtained through fitting of least–square curves using the program ORIGIN 8.5.

All theoretical calculations were performed with the ORCA 4.2.1 software [36].

The geometry of dye **7** was optimized at the Tao–Perdew–Staroverov–Scuseria (TPSS) density–functional level [37], employing the triple–ξ Karlsruhe basis set (def2–TZVP) [38]. Dispersion forces were accounted for with Grimme's D3 correction [39]. Frequencies were calculated for all molecules to ensure energy minima. Solvent effects were mimicked with the conductor–like polarizable continuum model (CPCM) approach [40]. Transition energies in each solvent were then obtained from time–dependent density functional theory (TD/DFT) calculations on the optimized geometries at the same level of theory, with the pure functional (PBE) [41], the range–separated hybrid functional ω–B97X–D3 [42], and the def2–TZVP basis set [38].

4. Results and discussion

4.1. Synthesis and characterization

Compounds **7**–**12** were synthesized following the methodology adapted from de Melo et al. 25. The corresponding Schiff bases were obtained through the condensation reaction of the corresponding amine with 5–nitro–2–thiophenecarboxaldehyde or 5–nitro–2–furaldehyde in the presence of dry ethanol and glacial acetic acid, with the consequent elimination of water (Scheme 1). Novel compounds **7**–**12** were fully characterized using IR, ^{1}H NMR, ^{13}C NMR, HRMS, and DSC techniques (Figs. S2–S31) and the products were obtained with yields ranging from 73 to 87%. The results show that all compounds were obtained with the required purity for the UV–vis spectrophotometric studies to be carried out.

4.2. Solvatochromic studies

Fig. 3 shows solutions and UV–vis spectra for compounds **7** (**A**) and **8** (**B**) in solvents of different polarities, which show that these dyes are solvatochromic, presenting different solution colors in solvents with different polarity. By comparison, compounds **9**–**12** exhibit a weaker solvatochromism (Figs. S32 and S33). The solvatochromic bands observed in the visible region of the spectrum of compounds **7**–**12** are the result of electronic transitions of the π–π* type, with a charge transfer from the electron–donor moiety (*N*,*N*–dimethylamino, methoxy or methylthio groups) to the electron–acceptor moiety (2–nitrothiophenyl or 2–nitrofuranyl). Taking compound **7** as an example, the λ_{max} of the solvatochromic band measured in *n*–hexane appears at 464 nm, while in diethyl ether, the band is displaced at $\lambda_{max} = 476$ nm ($\Delta\lambda_{max} = +12$ nm). In ethanol and DMSO, the λ_{max} is verified at 487 nm and 511 nm, respectively ($\Delta\lambda_{max} = +24$ nm). Compounds **8** and **11** show similar behavior, while the other compounds show only a very small variation in maximum absorption wavelengths in solvents with different polarities.

The UV–vis spectra for each compound in various solvents were used to obtain, through the first derivative, the λ_{max} values of the solvatochromic bands, which were used to calculate the corresponding E_T (dye) values in kcal mol^{-1}, using Eq. (1) (Table 1).

Fig. 4 shows the plots of the E_T (dye) obtained for compounds **7**–**12** in each of the solvents studied, as a function of E_T (30). Compounds **7**, **8**, and **11** exhibit a positive solvatochromic behavior. Taking compound **7** as an example, the solvatochromic band has a maximum at 464 nm [E_T (**7**) = 61.6 kcal mol^{-1}] in *n*–hexane, while in DMSO the $\lambda_{max} = 511$ nm [E_T (**7**) = 56.0 kcal mol^{-1}]. Thus, a reduction in the E_T (**7**) value by 5.6 kcal mol^{-1} occurs following an increase in the polarity of the medium, leading to a bathochromic change of $\Delta\lambda_{max} = +47$ nm, which is characteristic of positive solvatochromism. For compound **8**, considering the λ_{max} values in *n*–hexane (444 nm) and in benzyl alcohol (496 nm), a $\Delta\lambda_{max} = +52$ nm was verified.

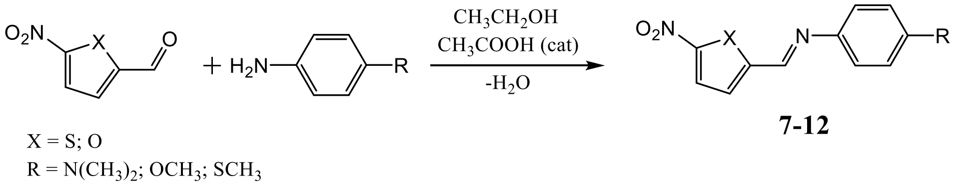

Scheme 1. Route for the synthesis of compounds **7**–**12** (see Fig. 2).

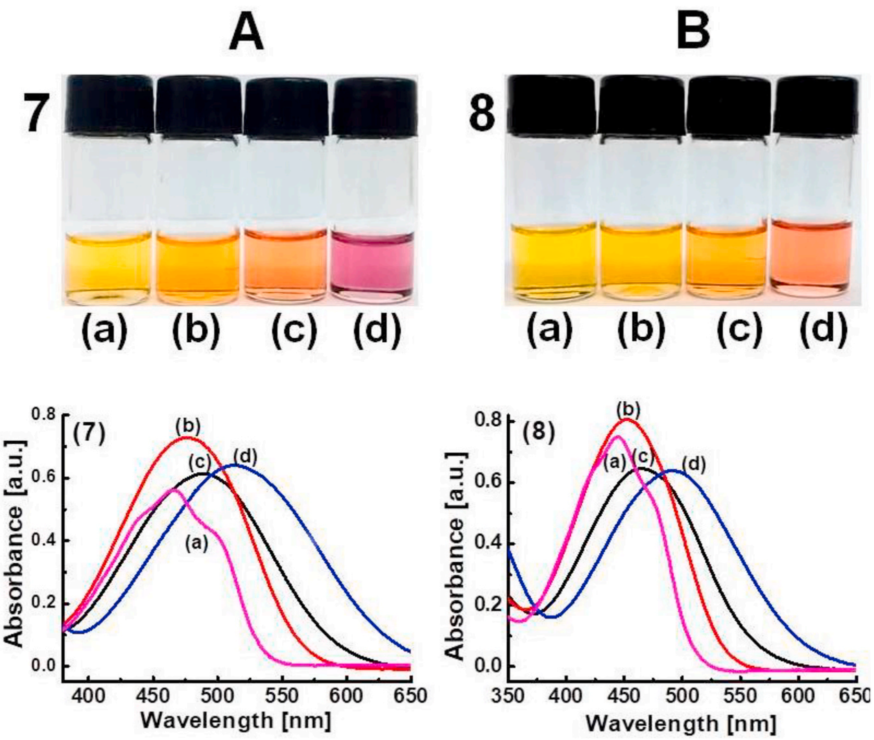

Fig. 3. Solutions and UV–vis spectra of dyes **7** **(A)** and **8** **(B)** in **(a)** *n*–hexane, **(b)** diethyl ether, **(c)** ethanol, and **(d)** DMSO.

It was also verified that in water, compounds **7** and **8** exhibit an anomalous behavior (red squares in Fig. 4), which does not follow the pattern presented in the other solvents. Therefore, the later studies using these compounds were carried out disregarding water. Probes **9**, **10**, and **12** exhibited a peculiar solvatochromism, because their experimental data ploted as a function of E_T (30) did not show any relationship.

Dye **2** is considerably more solvatochromic than compounds **7**–**12**, exhibiting a $\Delta\lambda_{max} = +97$ nm between the solvents DMSO and *n*–hexane. When considering formamide, which is a solvent that was not used in the study of compounds **7**–**12**, the variation becomes even larger ($\Delta\lambda_{max} = +111$ nm). The most solvatochromic of compounds **7**–**12** is dye **8**, with a 52 nm variation between the extremes (longer wavelength – shorter wavelength).

Despite the difference in the extent of solvatochromism, when considering the same solvents, the plots of E_T (dye) as a function of E_T (30) for compounds **7** and **8** are very similar to dye **2** (Fig. S34), with emphasis for dye **7**, which has the same electron–acceptor (5–nitro–2–thiophenyl) and electron–donor (dimethylamino) moieties. This fact shows that the structural similarities between the compounds are reflected in their interactions with the medium.

Fig. 5 shows plots of E_T values for dyes **7**–**12** as a function of E_T (**2**). This type of plot is used to verify the similarities of the probes studied with respect to the given standard probe **2** [24–27]. Data were treated using Eq. (2), where m measures the average shift of the λ_{max} value for a solvatochromic dye with respect to standard **2** while n compares the solvatochromic sensitivity of the dye to solvent polarity changes with that of probe **2**.

$$E_T\ (\text{dye}) = \text{m} + \text{n}\ E_T\ (\mathbf{2}) \tag{2}$$

Data show that the E_T values for dyes **7**, **8**, and **11** match reasonably well with those of standard **2** ($r^2 > 0.78$), while the other dyes provide $r^2 < 0.62$ (Table S1). Positive values of m (>28) are obtained for the dyes studied, indicating that the solvatochromic band of these probes is hypsochromically shifted in comparison with the vis band of standard probe **2**. The analysis of n values show that all dyes studied are solvatochromically less sensitive than dye **2**, with the best results being verified for dyes **7** (n = 0.50), **8** (n = 0.58), and **11** (n = 0.44).

4.3. Multiparametric analysis

The experimental E_T (dye) values for compounds **7**–**12** in pure solvents were analyzed using the Kamlet–Abboud–Taft (KAT) [43,44] and Catalán [30] multiparametric equations. The KAT approach uses Eq. (3), where α, β, and π^* are parameters that represent the solvent hydrogen–bond donor (HBD) acidity, hydrogen–bond acceptor (HBA) basicity, and solvent dipolarity/polarizability, respectively, while δ is a polarizability correction term for the solvent. The Catalán approach [30] requires the use of Eq. (4), where specific solvent parameters *SA* and *SB* represent the solvent HBD acidity and HBA basicity, respectively, while *SP* and *SdP* are the nonspecific solvent parameters polarizability and dipolarity, respectively. In these equations, E_T (dye)$_0$ represents the E_T (dye) value in the gas phase and a, b, c, d, and s are regression

Table 1
E_T (30) and E_T (dye) values given in kcal mol^{-1} for compounds **2** and **7**–**12** for 29 solvents.

Solvent	E_T (30)[a]	2[b]	7	8	9	10	11	12
Cyclohexane	30.9	60.6	60.7	63.5	69.9	73.3	71.5	70.8
***n*–Hexane**	31.0	61.3	61.6	64.5	70.1	73.7	71.8	71.5
Toluene	33.9	56.3	58.6	61.4	68.7	73.1	67.6	70.2
Diethyl ether	34.5	57.6	60.1	63.2	70.1	73.1	69.4	72.2
THF	37.4	54.9	57.9	61.3	69.2	72.4	68.4	71.7
Ethyl acetate	38.1	55.7	58.8	62.3	70.1	72.9	69.7	72.4
1,2–Dimethoxyethane	38.2	[c]	58.5	61.9	69.4	72.8	68.7	71.7
Trichloromethane	39.1	53.9	57.4	59.2	69.1	71.7	[d]	[d]
Acetophenone	40.6	[c]	56.1	58.3	69.2	70.9	67.3	70.4
Dichloromethane	40.7	53.4	57.3	59.1	68.7	71.3	67.8	70.1
1,2–Dichloroethane	41.3	53.3	57.2	59.1	68.7	71.1	67.4	69.9
Acetone	42.2	54.1	58.1	61.4	69.9	72.9	68.9	72.0
DMA	42.9	[c]	56.6	59.2	68.4	71.3	67.6	70.2
DMF	43.2	52.1	56.7	59.4	68.6	70.9	67.4	70.2
2–Methylpropan–2–ol	43.3	55.7	59.0	62.1	70.1	72.8	69.2	71.5
DMSO	45.1	50.6	56.0	58.1	67.9	70.6	66.8	69.4
Acetonitrile	45.6	53.6	58.2	61.0	69.9	72.8	68.9	71.7
Butan–2–ol	47.1	[c]	58.6	61.4	69.7	72.8	68.6	71.5
Decan–1–ol	47.7	[c]	58.5	61.4	69.4	72.6	68.2	70.8
Octan–1–ol	48.1	[c]	58.7	61.2	69.2	72.4	68.1	70.8
Propan–2–ol	48.4	55.4	58.7	61.8	69.9	72.9	68.9	71.7
Pentan–1–ol	49.1	[c]	58.5	61.1	69.2	72.8	68.6	71.5
Butan–1–ol	49.7	55.3	58.3	57.7	69.9	72.8	68.4	71.1
Benzyl alcohol	50.4	[c]	56.1	61.1	68.2	70.6	67.0	68.9
Propan–1–ol	50.7	[c]	58.3	61.5	69.7	72.8	68.7	71.5
Ethanol	51.9	55.0	58.7	61.5	69.7	72.9	69.1	71.7
Methanol	55.4	54.5	58.6	61.5	70.1	73.1	69.4	71.8
Ethane–1,2–diol	56.3	[c]	56.6	58.8	69.9	72.2	67.8	70.9
Water	63.1	[c]	62.3	63.9	70.6	72.9	66.5	71.5

[a] Values obtained from Reichardt [1].

[b] Values obtained from Effenberger et al. [6,7].

[c] Value not found.

[d] Insoluble.

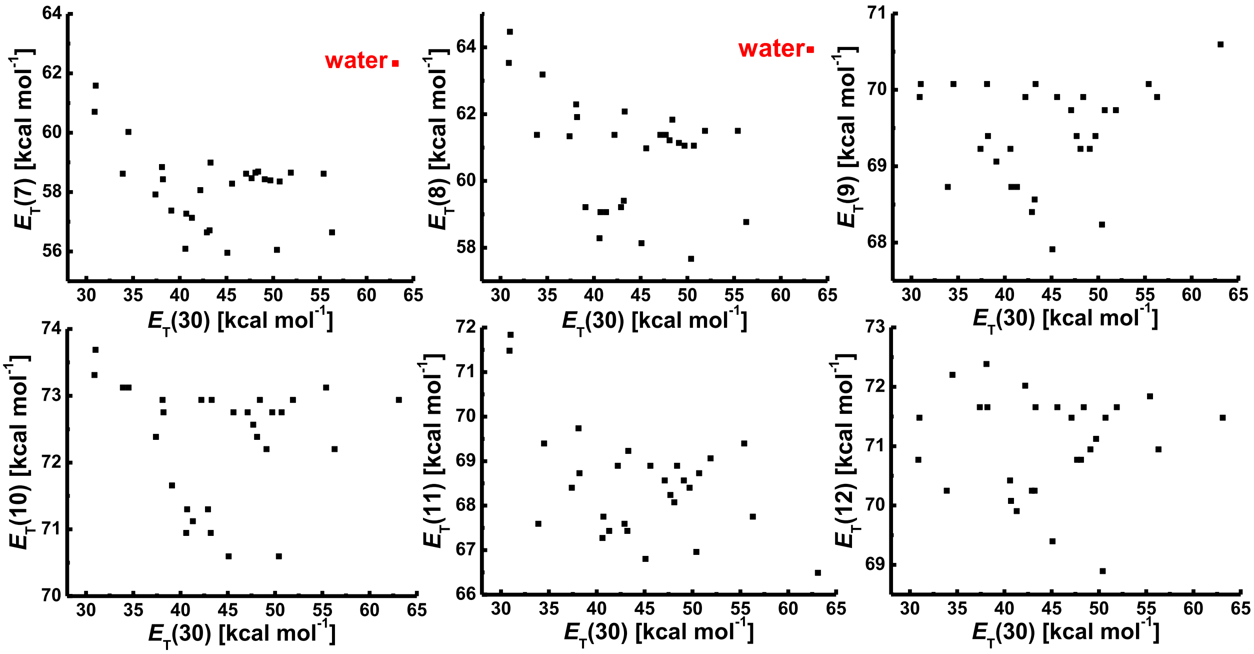

Fig. 4. E_T (dye) value as a function of E_T (30) for dyes **7**–**12**.

coefficients that reflect the relative importance of the solvent parameters in terms of E_T (dye).

$$E_T\ (\text{dye}) = E_T\ (\text{dye})_0 + a\alpha + b\beta + s\ (\pi^* + d\delta) \tag{3}$$

$$E_T\ (\text{dye}) = E_T\ (\text{dye})_0 + a SA + b SB + c SP + d SdP \tag{4}$$

Tables 2 and Table S2 show the contributions of solvent properties to the E_T (dye) values for compounds **7**–**12**, using the Catalán and KAT equations, respectively. Table 2 also shows the results obtained when applying Eq. (4) to the literature data referring to dyes **2** [6,7], **13**, and **14** (Fig. 6). Compound **13** was proposed by Catalán as a probe for the polarizability of the medium, being used as the descriptor of Eq. (4)

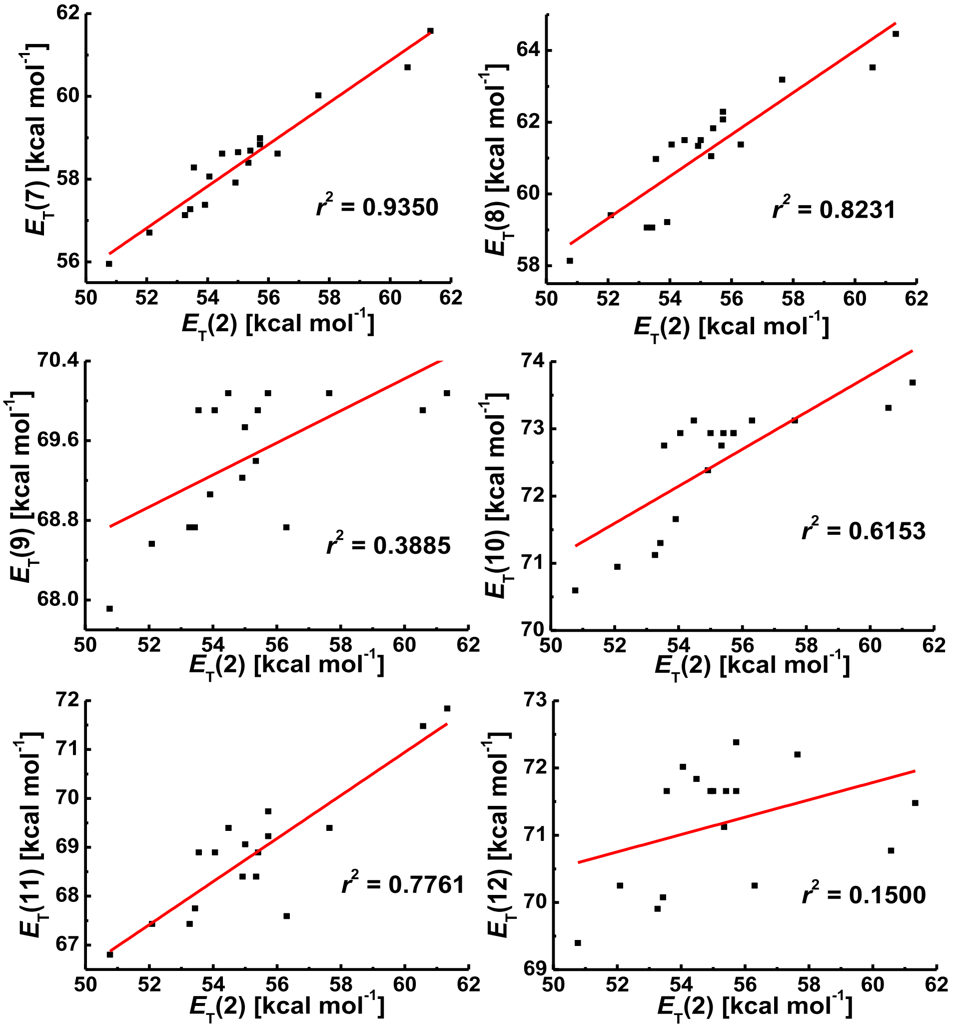

Fig. 5. Comparison between E_T (**dye**) and E_T (**2**) for compounds **7**–**12**.

Table 2

Regression coefficients a, b, c, and d obtained from the Catalán multiparametric analysis through the treatment of E_T (dye) values for dyes **1**, **2**, and **7**–**14** in pure solvents.

Dye	E_T (dye)$_0$	a	b	c	d	*N*	*r*	S.D.
1[a,b]	30.3	24.0	4.14	1.12	9.44	28	0.97	1.61
2[b]	70.1	0.01	0.06	−14.6	−7.32	18	0.99	0.32
7[c]	68.8	−0.03	−0.35	−12.1	−2.89	28	0.99	0.15
8[c]	74.5	−1.04	0.34	−16.5	−3.06	28	0.98	0.30
9[c]	74.7	0.74	−0.41	−7.14	−0.22	28	0.86	0.34
10[c]	79.8	0.61	−0.25	−9.40	−1.22	28	0.93	0.35
11[c]	78.6	0.26	−1.21	−11.8	−1.61	28	0.93	0.48
12[c]	78.2	−0.38	0.15	−10.5	−0.29	28	0.89	0.43
13[d]	68.5	−0.005	0.002	−10.1	0.001	38	1.00	0.002
14[e]	70.3	0.17	−0.007	−11.1	−0.03	38	0.98	0.10

[a] Using E_T (30) values from Table 1 [1].

[b] Using E_T (**2**) values from Table 1 [6,7].

[c] Excluding water.

[d] Using data from Catalán, 2009 [30].

[e] Using data from El Seoud et al., 2013 [31].

[30]. Later, El Seoud et al. proposed the use of β–carotene (**14**) to determine the polarizability of the medium due to the structural similarity of the latter with probe **13** [31,32]. Catalán argued that the solvatochromism of β–carotene is governed predominantly by the polarizability of the medium, but the contribution of other solute/solvent interactions, such as acidity and dipolarity cannot be neglected [33].

Eq. (4) is better applied than Eq. (3) to the studied compounds, since provided higher correlation coefficients (*r*) and lower values of standard deviation (S.D.). The analysis of the data obtained with both equations show that the polarizability represents the most influential solvent descriptor in the solvation of dyes **7**–**12**, given the larger magnitude of

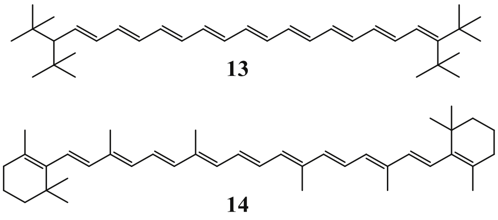

Fig. 6. Molecular structures of compounds **13** and **14**.

their correlation coefficients when Eq. (4) is applied.

Considering the data generated with Eq. (4), it is also important to note that, in general, the other solvent parameters have only little influence on the dye solvation and that, although small, they should have similar importance, considering that the magnitude of all values obtained is quite similar and does not follow a pattern for each regression coefficient, considering different dyes. An exception is the sensitivity of compound **12**, showing that the regression coefficients related to HBD acidity, HBA basicity, and dipolarity are close to zero and can be neglected. Thus, dye **12** probes practically only the polarizability of the medium.

Data obtained from applying Eq. (4) show that dye **2** is also sensitive to the HBD acidity of the medium, but its sensitivity is low. Therefore, it is possible to say that dye **2** interacts in a specific way with the medium, but with little intensity [6,7]. Furthermore, when comparing the values of the regression coefficients generated for dyes **2**, **7**, and **8**, it is found that their interactions with the medium are quite similar, but compounds **7** and **8** interact less strongly with the HBD acidity and the HBA basicity of the solvents, considering that the magnitude of the regression coefficient related to these parameters is lower, especially for dye **7**.

Regarding the signs obtained for each regression coefficient, all or almost all values are negative for compounds **2**, **7**, **8**, and **11**. This is an intrinsic characteristic for results of applying Eq. (4) for compounds that exhibit positive solvatochromic behavior. For compounds **9** and **10**, the regression coefficients a, related to HBD acidity, have a positive value whereas the others have a negative value. However, the values of coefficients a are very low, which does not constitute a reverse solvatochromism, but a positive solvatochromism. Compound **12** has almost all negative signs, only the coefficient b related to HBA basicity being positive.

In order to confirm that the polarizability/dipolarity of the solvents is the predominant factor in the solvation of the dyes, Eq. (4) was applied excluding one parameter at a time. The results obtained for compounds **1**, **2**, **7**, and **8** are compiled in Table 3 and for compounds **9**–**12** are listed in Table S3. These data confirm that the solvent's polarizability is the most influential parameter for the solvation of compounds **7**–**12**, since by excluding it from the calculation with the Catalán multiparametric equation, the lowest correlation coefficients and the highest standard deviations are obtained.

The results also show that for compounds **7**–**12** the solvent's dipolarity parameter is the second most important factor for the solvation of compounds, since the correlation coefficients have a small decrease when this parameter is disregarded in the application of Eq. (4). When dealing with compound **12** (Table S3), the results obtained from applying Eq. (4), excluding one parameter at a time, confirm that we are indeed facing a solvatochromic dye that probes mainly the polarizability of the medium, considering that the correlation coefficient is not affected when the other parameters are disregarded in the regression analysis. In addition, the E_T (**12**) values match reasonably well with SP, with $r^2 > 0.779$ (Fig. S35; Table S4), which is a value close to that obtained when all parameters of Eq. (4) are utilized ($r^2 > 0.89$). This result is interesting because it points to the possibility of designing easily accessible polarizability probes with an entirely different skeleton from other polarizability probes, such as the polyenes **13** and **14**.

In general, probes **7**–**12** are poorly sensitive to the medium acidity and basicity and much more sensitive to the medium dipolarity and polarizability, being more sensitive to solvent polarizability. In particular, compounds **7** and **12** are practically not sensitive to the HBD acidity and HBA basicity of the medium, both compounds being very sensible to the polarizability in comparison with the dipolarity of the medium: the **c**/**d** ratios are 4.2 and 32.4 for dyes **7** and **12**, respectively. The results shown here also illustrate the importance of electron donor groups to tailor the level of interaction of the probes with the medium. The combination of electron donating capacity and greater polarizability of the *N*,*N*–dimethylamino and methylthio groups, in comparison with the methoxy group, seems to be a determining factor to explain the extent of solvatochromism exhibited by the probes.

Table 3
Influence of each solvent parameter in the Catalán multiparametric analysis on the fitting of data for dyes **1**, **2**, **7**, and **8** (excluding water).

Dye	E_T (dye)$_0$	a	b	c	d	N	r	S.D.
1	30.3	24.0	4.14	1.12	9.40	28	0.97	1.61
	29.1	–	10.7	0.81	12.2	28	0.74	4.82
	26.8	25.9	6.94	12.3	–	28	0.91	2.85
2	70.1	0.01	0.06	−14.6	−7.32	18	0.99	0.32
	60.1	2.26	−1.50	–	−8.98	18	0.94	0.97
	77.0	−3.36	−4.03	−28.4	–	18	0.75	1.89
7	68.8	−0.03	−0.35	−12.1	−2.90	28	0.99	0.15
	64.4	−0.01	0.80	–	−4.03	28	0.75	0.87
	69.9	−0.61	−1.20	−15.5	–	28	0.84	0.84
8	74.5	−1.04	0.34	16.5	−3.06	28	0.98	0.30
	63.0	−1.01	1.92	–	−4.62	28	0.73	1.21
	75.6	−1.67	−0.56	−20.1	–	28	0.88	0.83

4.4. Theoretical calculations

In search of theoretical support to the spectral data obtained for solvatochromic dyes **7**–**11**, compound **7** was chosen for theoretical studies because of its analogy with reference compound **2**, evident from the good correlation of its solvatochromic E_T (**7**) values with those of reference **2** (Fig. 5). Our theoretical experience with Effenberger's dye **2**, which shows a positive solvatochromism that could be qualitatively reproduced with the aid of implicit solvation models coupled with TD/DFT methods [11], led us to employ the same methodology for the calculation of the absorption energies of the solvatochromic band of **7**. Structure **7** was first optimized in ten different solvents, employing a DFT/TPSS/def2–TZVP method [38] and the CPCM approach [40] as an implicit model to mimic solvent effects.

Fig. 7 reproduces its HOMO and LUMO densities calculated in DMSO. The solvatochromic band of the dye is associated with an internal charge–transfer transition from the electron–donor *N*,*N*–dimethylaminophenyl to the electron–acceptor 5–nitrothienyl group through an imino bridge. This transition is solvent–dependent, as can be seen by the values of E_T (**7**) calculated in ten different solvents of increasing dielectric permittivity (ε), listed in Table 4. E_T (**7**) values were obtained by TD/DFT calculations on the optimized structures in each solvent, employing two different functionals, PBE [41] and ω–B97X–D3 [42]. For the sake of comparison, experimental E_T (**7**) values in the same solvents are also reproduced in Table 4.

TD/DFT calculations offer the advantage of being rather inexpensive and providing transition energies with reasonable errors [45]. A major shortcoming of this rather popular method is its poor ability to reproduce accurate charge–transfer transitions. In addition, errors vary widely, depending on the functional employed in the calculation. This had been observed by us in a recent paper, where the effectiveness of continuum models to mimic solvent effects was evaluated for three dyes with a solvatochromic behavior that was strongly, or solely dependent on the medium polarizability and dipolarity [11].

Traditionally regarded as non–specific solvent properties, the variation of the medium polarizability and dipolarity should be adequately

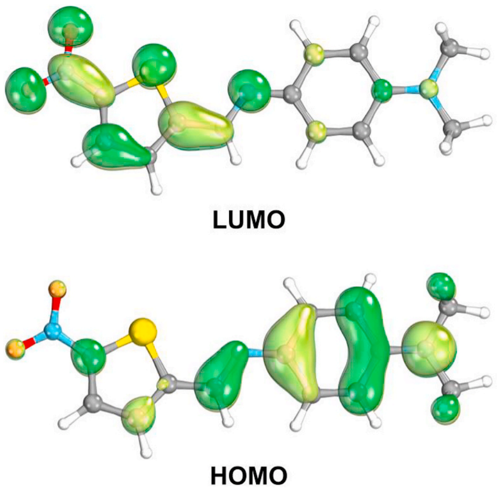

Fig. 7. Frontier molecular orbitals of dye **7** obtained with a DFT/ω–B97X–D3/def2–TZVP method (CPCM = DMSO).

described by a continuum model. Calculations with a TD/DFT method in ten solvents and employing eleven different functionals showed that this is not true. Depending on the employed functional, the calculated transition energies do not only depart from the experimental values, when employing a continuum model, but also yield opposite solvatochromic trends. The use of molecular simulations with the introduction of explicit solvent molecules in the calculations yields significantly better results [11].

The results of the present study confirm these findings. Table 4 shows that the differences between the calculated and experimental E_T (**7**) values in the ten solvents were in the range of 0.24–0.37 eV, with an average value of 0.26 eV. This average value is thus within the range of 0.2–0.4 eV reported by Jacquemin et al. for errors by TD/DFT calculations [45]. In addition, the two methods yield opposite predictions regarding the solvatochromism of **7**. This is readily seen by inspection of Fig. 8, where calculations employing the ω–B97X–D3/def2–TZVP method yield a positive solvatochromism for dye **7**, in agreement with its behavior and with that of its analog **2**. An opposite trend is predicted by the PBE/def2–TZVP method, which thus departs also qualitatively from the behavior of dye **7**.

Following our previous conclusions [11], the different performance of the two methods can be attributed to the different degrees of long–range Hartree–Fock (HF) exchange present in the calculations. PBE is a method completely devoid of HF exchange [41], whereas the ω–B97X–D3/def2–TZVP method comprises nearly 20% short–range and 100% long–range HF exchange [42]. The results of the present study reinforce our observations that functionals with little or no HF exchange are less effective in reproducing the positive solvatochromism of dipolar and polarizable dyes.

5. Conclusions

Dyes **7**–**11** were synthesized and characterized. Compounds **7** and **8** are solvatochromic and therefore exhibit different colors in various solvents, while in comparison dyes **9**–**12** exhibit only a weak solvatochromism. Probes **7**, **8**, and **11** present a behavior very similar to Effenberger's dye (**2**), showing a positive solvatochromic behavior. The application of multiparametric equations shows that polarizability is the most influential solvent parameter in the solvation of the dyes studied. In addition, the multiparametric analysis utilizing the Catalán approach confirms the similarity of dyes **7**, **8**, and **11** with dye **2** concerning the interactions that the dyes experience with the medium. In addition, dye **12** is an excellent probe for the polarizability of the medium since it is not sensitive to any other parameter of the solvent. Theoretical calculations were performed with dye **7** in ten different solvents, employing a continuum model to mimic solvent effects and TD/DFT calculations with two functionals exhibiting a different degree of Hartree–Fock

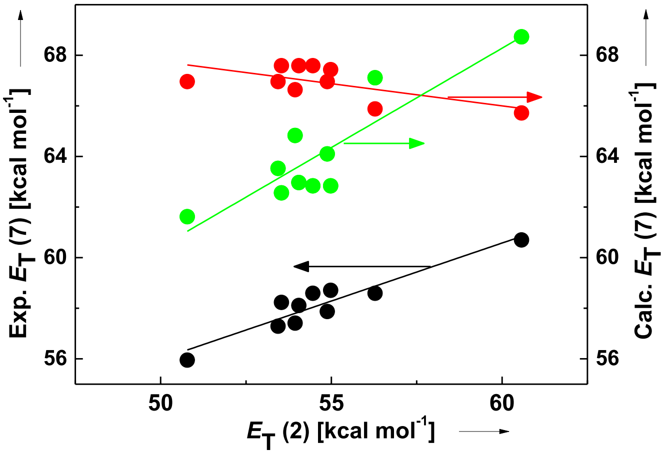

Fig. 8. Transition energies of dye **7** in ten different solvents, plotted against the experimental transition energies of reference dye **2** [6,7]. Experimental E_T (**7**) values (black circles) are compared with calculated E_T (**7**) values by the PBE/def2–TZVP (red circles) and the ω–B97X–D3/def2–TZVP (green circles) methods. (For interpretation of the references to color in this figure legend, the reader is referred to the Web version of this article.)

Table 4

Solvent–dependent transition energies of dye **7**, calculated by CPCM in ten solvents of increasing dielectric permittivity (ε), with two different TD/DFT methods, employing the PBE/def2–TZVP and the ω–B97X–D3/def2–TZVP functionals.

Solvent (ε)[a]	Calculated E_T (7) value[b]		Exp. E_T (7) value[b]	ΔE_T[b,c]
	PBE	ω–B97X–D3		
Cyclohexane (2.02)	66.18 (2.87)	68.73 (2.98)	60.7 (2.63)	8.03 (0.35)
Toluene (2.38)	65.86 (2.86)	67.11 (2.91)	58.6 (2.54)	8.52 (0.37)
Trichloromethane (4.81)	66.64 (2.89)	64.83 (2.81)	57.4 (2.49)	7.42 (0.32)
THF (7.25)	66.96 (2.90)	64.10 (2.78)	57.9 (2.51)	6.23 (0.27)
Dichloromethane (9.08)	66.96 (2.90)	63.53 (2.76)	57.3 (2.48)	6.24 (0.28)
Acetone (20.49)	67.59 (2.93)	62.97 (2.73)	58.1 (2.52)	4.86 (0.21)
Ethanol (24.3)	67.43 (2.92)	62.84 (2.72)	58.7 (2.55)	4.13 (0.17)
Methanol (32.63)	67.59 (2.93)	62.84 (2.72)	58.6 (2.54)	4.25 (0.18)
Acetonitrile (36.6)	67.59 (2.93)	62.56 (2.71)	58.2 (2.53)	4.33 (0.18)
DMSO (47.0)	66.96 (2.90)	61.62 (2.67)	56.0 (2.43)	5.67 (0.24)

[a] Permittivity constants used in the calculations are given between brackets.

[b] In kcal mol^{-1} and, between brackets, in eV.

[c] Error difference between calculated (ω–B97X–D3/def2–TZVP) and experimental values. Conversion factors: 1 kcal mol^{-1} = 4.2 kJ mol^{-1}; 1 eV = 96 kJ mol^{-1}

exchange to estimate transition energies. A HOMO–LUMO transition involving an internal charge transfer from the *N*,*N*–dimethylaminophenyl electron–donor to the nitrothienyl electron–acceptor group was identified as the origin of the solvatochromic band of **7**. Although with an average error of 0.26 eV from the experimental transition energies, the calculated E_T (**7**) values reproduce qualitatively the positive solvatochromism of this dye in ten solvents. Thus, the study reported here illustrates the potential of new solvatochromic compounds inspired in the Effenberger's dye, with easy synthetic access, for probing the polarizability of microenvironments.

Author contribution statement

Carlos E. A. de Melo: methodology, investigation, writing – original draft; Moisés Domínguez: conceptualization, methodology, investigation, writing–original draft; Marcos C. Rezende: conceptualization, methodology, writing–original draft; Vanderlei G. Machado: conceptualization, methodology, supervision, funding acquisition, project administration, writing–original draft, and writing–review & editing.

Declaration of competing interest

The authors declare that they have no known competing financial interests or personal relationships that could have appeared to influence the work reported in this paper.

Acknowledgements

The financial support of the Brazilian Conselho Nacional de Desenvolvimento Científico e Tecnológico (CNPq), Coordenação de Aperfeiçoamento de Pessoal de Nível Superior (CAPES – Finance code 001), Fundação de Amparo à Pesquisa e Inovação do Estado de Santa Catarina (FAPESC), Laboratório Central de Biologia Molecular (CEBIME/UFSC), and UFSC is gratefully acknowledged. Thanks are also due to Fondecyt project 1190045.

Appendix A. Supplementary data

Supplementary data to this article can be found online at https://doi.org/10.1016/j.dyepig.2020.108757.

References

[1] Reichardt C. Solvatochromic dyes as solvent polarity indicators. Chem Rev 1994;94:2319–58. https://doi.org/10.1021/cr00032a005.

[2] Suppan P, Ghoneim N. Solvatochromism. Cambridge, UK: Royal Society of Chemistry; 1997.

[3] Reichardt C, Welton T. Solvents and solvent effects in organic chemistry. fourth ed. Weinheim, Germany: Wiley–VCH; 2011.

[4] Dimroth K, Reichardt C, Siepmann T, Bohlmann F. Über Pyridinium–*N*–phenol–betaine und ihre Verwendung zur Charakterisierung der Polarität von Lösungsmitteln. Justus Liebigs Ann Chem 1963;661:1–37. https://doi.org/10.1002/jlac.19636610102.

[5] Machado VG, Stock RI, Reichardt C. Pyridinium *N*–phenolate betaine dyes. Chem Rev 2014;114:10429–75. https://doi.org/10.1021/cr5001157.

[6] Effenberger F, Würthner F. 5–Dimethylamino–5′–nitro–2, 2′–bithiophene – a new dye with pronounced positive Solvatochromie. Angew Chem Int Ed 1993;32:719–21. https://doi.org/10.1002/anie.199307191. 5–Dimethylamino–5'–nitro–2,2'–bithiophen – ein neuer Farbstoff mit ausgeprägter positiver solvatochromie. Angew Chem 1993;105:742–4, 10.1002/ange.19931050515.

[7] Effenberger F, Würthner F, Steybe F. Synthesis and solvatochromic properties of donor–acceptor–substituted oligothiophenes. J Org Chem 1995;60:2082–91. https://doi.org/10.1021/jo00112a032.

[8] Ramirez CB, Carrasco N, Rezende MC. Halochromism and solvatochromism of a π* probe in binary solvent mixtures. J Chem Soc, Faraday Trans 1995;91:3839–42. https://doi.org/10.1039/ft9959103839.

[9] Dominguez ME, Rezende MC, Marquez S. Theoretical study of the solvatochromism of a donor–acceptor bithiophene. J Mol Model 2013;19:689–96. https://doi.org/10.1007/s00894–012–1593–y.

[10] Dominguez M, Mera–Adasme R, Rezende MC. Insights into the halochromism of a bithiophene π* probe. Spectrochim Acta, Part A 2019;222. https://doi.org/10.1016/j.saa.2019.117264. 117264.

[11] Mera–Adasme R, Rezende MC, Dominguez M. On the physical–chemical nature of solvent polarizability and dipolarity. Spectrochim Acta, Part A 2020;229. https://doi.org/10.1016/j.saa.2019.118008. 118008.

[12] Brooker LGS, Keyes GH, Heseltine DW. Color and constitution. XI.1 Anhydronium bases of *p*–hydroxystyryl dyes as solvent polarity indicators. J Am Chem Soc 1951;73:5350–6. https://doi.org/10.1021/ja01155a097.

[13] Brooker LGS, Keyes GH, Sprague RH, VanDyke RH, VanLare E, VanZandt G, et al. Studies in the cyanine dye series. XI.1 the merocyanines. J Am Chem Soc 1951;73:5326–32. https://doi.org/10.1021/ja01155a097.

[14] Benson HG, Murrell JN. Some studies of benzenoid–quinonoid resonance .2. Effect of solvent polarity on structure and properties of merocyanine dyes. J Chem Soc Faraday Trans II 1972;68:137–43. https://doi.org/10.1039/f29726800137.

[15] Botrel A, le Beuze A, Jacques P, Strub H. Solvatochromism of a typical merocyanine dye. A theoretical investigation through the CNDO/SCI method including solvation. J Chem Soc, Faraday Trans 2 1984;80:1235–52. https://doi.org/10.1039/f29848001235.

[16] Jacques P. On the relative contributions of nonspecific and specific interactions to the unusual solvatochromism of a typical merocyanine dye. J Phys Chem 1986;90:5535–9. https://doi.org/10.1021/j100280a012.

[17] Cavalli V, da Silva DC, Machado C, Machado VG, Soldi V. The fluorosolvatochromism of Brooker's merocyanine in pure and in mixed solvents. J Fluoresc 2006;16:77–86. https://doi.org/10.1007/s10895–005–0053–9.

[18] Murugan NA, Kongsted J, Rinkevicius Z, Agren H. Demystifying the solvatochromic reversal in Brooker's merocyanine dye. Phys Chem Chem Phys 2011;13:1290–2. https://doi.org/10.1039/c0cp01014f.

[19] Silva DL, Murugan NA, Kongsted J, Agren H, Canuto S. Self–aggregation and optical absorption of stilbazolium merocyanine in chloroform. J Phys Chem B 2014;118:1715–25. https://doi.org/10.1021/jp411178h.

[20] de Melo CEA, Nandi LG, Domínguez M, Rezende MC, Machado VG. Solvatochromic behavior of dyes with dimethylamino electron–donor and nitro electron–acceptor groups in their molecular structure. J Phys Org Chem 2015;28:250–60. https://doi.org/10.1002/poc.3402.

[21] Nandi LG, Facin F, Marini VG, Zimmermann LM, Giusti LA, Silva R, et al. Nitro–substituted 4–[(phenylmethylene)imino]phenolates: solvatochromism and their use as solvatochromic switches and as probes for the investigation of preferential solvation in solvent mixtures. J Org Chem 2012;77:10668–79. https://doi.org/10.1021/jo301890r.

[22] Stock RI, Nandi LG, Nicoleti CR, Schramm ADS, Meller SL, Heying RS, et al. Synthesis and solvatochromism of substituted 4–(nitrostyryl)phenolate dyes. J Org Chem 2015;80:7971–83. https://doi.org/10.1021/acs.joc.5b00983.

[23] Stock RI, Schramm ADS, Rezende MC, Machado VG. Reverse solvatochromism in solvent binary mixtures: a case study using a 4–(nitrostyryl)phenolate as a probe. Phys Chem Chem Phys 2016;18:20266–9. https://doi.org/10.1039/c6cp03875a.

[24] Stock RI, de Melo CEA, Schramm ADS, Nicoleti CR, Bortoluzzi AJ, Heying RS, et al. Structure–behavior study of a family of "hybrid cyanine" dyes which exhibit inverted solvatochromism. Phys Chem Chem Phys 2016;18:32256–65. https://doi.org/10.1039/c6cp06708e.

[25] deMelo CEA, Nicoleti CR, Rezende MC, Bortoluzzi AJ, Heying RdaS, Oliboni RdaS, et al. Reverse solvatochromism of imine dyes comprised of 5–nitrofuran–2–yl or 5–nitrothiophen–2–yl as electron acceptor and phenolate as electron donor. Chem Eur J 2018;24:9364–76. https://doi.org/10.1002/chem.201800613.

[26] Stock RI, Sandri C, Rezende MC, Machado VG. Solvatochromic behavior of substituted 4–(nitrostyryl)phenolate dyes in pure solvents and in binary solvent mixtures composed of water and alcohols. J Mol Liq 2018;264:327–36. https://doi.org/10.1016/j.molliq.2018.05.042.

[27] de Melo CEA, Nicoleti CR, Nandi LG, Schneider FSS, Oliboni RD, Caramori GF, et al. Solvatochromism of new substituted 4–(*E*)–(4–nitrophenyl)diazenyl phenolate dyes. J Mol Liq 2020;301:12. https://doi.org/10.1016/j.molliq.2019.112330.

[28] Catalán J, Hopf H. Empirical treatment of the inductive and dispersive components of solute–solvent interactions: the solvent polarizability (SP) scale. Eur J Org Chem 2004:4694–702. https://doi.org/10.1002/ejoc.200400311.

[29] Catalán J, Hopf H, Mlynek C, Klein D, Kilickiran P. Electronic energy levels in all–trans long linear polyenes: the case of the 3,20–di(tert–butyl)–2,2,21,21–tetramethyl–all–trans–3,5,7,9,11,13,15,17, 19–docosanonaen (ttbp9) conforming to Kasha's rule. Chem Eur J 2005;11:3915–20. https://doi.org/10.1002/chem.200401093.

[30] Catalán J. Toward a generalized treatment of the solvent effect based on four empirical scales: dipolarity (SdP, a new scale), polarizability (SP), acidity (SA), and basicity (SB) of the medium. J Phys Chem B 2009;113:5951–60. https://doi.org/10.1021/jp8095727.

[31] Loffredo C, Pires PAR, Imran M, El Seoud OA. β–Carotene: a green, inexpensive, and convenient solvatochromic probe for the determination of solvent polarizability. Dyes Pigments 2013;96:16–24. https://doi.org/10.1016/j.dyepig.2012.07.017.

[32] Pires PAR, Imran M, Loffredo C, Donate PM, Previdi D, El Seoud OA. Solvatochromism of 2–(*N,N*–dimethylamino)–7–nitrofluorene and the natural dye *β*–carotene: application for the determination of solvent dipolarity and polarizability. J Phys Org Chem 2013;26:280–5. https://doi.org/10.1002/poc.3083.

[33] Catalán J. On the use of *β*–carotene as a probe for solvent polarizability. J Phys Org Chem 2013;26:948–52. https://doi.org/10.1002/poc.3201.

[34] Vogel AI, Tatchell AR, Furniss BS, Hannaford AJ, Smith PWG. Vogel's textbook of practical organic chemistry. fifth ed. Prentice Hall; 1996.

[35] Bradley D, Williams G, Lawton M. Drying of organic solvents: quantitative evaluation of the efficiency of several desiccants. J Org Chem 2010;75:8351–4. https://doi.org/10.1021/jo101589h.

[36] Neese F. Software update: the ORCA program system, version 4.0. WIREs Comput Mol Sci 2018;8:e1327. https://doi.org/10.1002/wcms.1327.

[37] Tao JM, Perdew JP, Staroverov VN, Scuseria GE. Climbing the density functional ladder: nonempirical meta–generalized gradient approximation designed for molecules and solids. Phys Rev Lett 2003;91. https://doi.org/10.1103/PhysRevLett.91.146401. 146401.

[38] Weigend F, Ahlrichs R. Balanced basis sets of split valence, triple zeta valence and quadruple zeta valence quality for H to Rn: design and assessment of accuracy. Phys Chem Chem Phys 2005;7:3297–305. https://doi.org/10.1039/b508541a.

[39] Grimme S, Antony J, Ehrlich S, Krieg H. A consistent and accurate ab initio parametrization of density functional dispersion correction (DFT–D) for the 94 elements H–Pu. J Chem Phys 2010;132. https://doi.org/10.1063/1.3382344. 154104.

[40] Barone V, Cossi M. Quantum calculation of molecular energies and energy gradients in solution by a conductor solvent model. J Phys Chem A 1998;102: 1995–2001. https://doi.org/10.1021/jp9716997.

[41] Perdew JP, Burke K, Ernzerhof M. Generalized gradient approximation made simple. Phys Rev Lett 1996;77:3865–8. https://doi.org/10.1103/PhysRevLett.77.3865.

[42] Lin YS, Li GD, Mao SP, Chai JD. Long–range corrected hybrid density functionals with improved dispersion corrections. J Chem Theor Comput 2013;9:263–72. https://doi.org/10.1021/ct300715s.

[43] Kamlet MJ, Taft RW. The solvatochromic comparison method. I. The *β*–scale of solvent hydrogen–bond acceptor (HBA) basicities. J Am Chem Soc 1976;98: 377–83. https://doi.org/10.1021/ja00418a009.

[44] Kamlet MJ, Abboud JLM, Abraham MH, Taft RW. Linear solvation energy relationships. 23. A comprehensive collection of the solvatochromic parameters, π*, α, and β, and some methods for simplifying the generalized solvatochromic equation. J Org Chem 1983;48:2877–87. https://doi.org/10.1021/jo00165a018.

[45] Loos P-F, Scemama A, Jacquemin D. The quest for highly accurate excitation energies: a computational perspective. J Phys Chem Lett 2020;11:2374–83. https://doi.org/10.1021/acs.jpclett.0c00014.